ChemComm

Accepted Manuscript

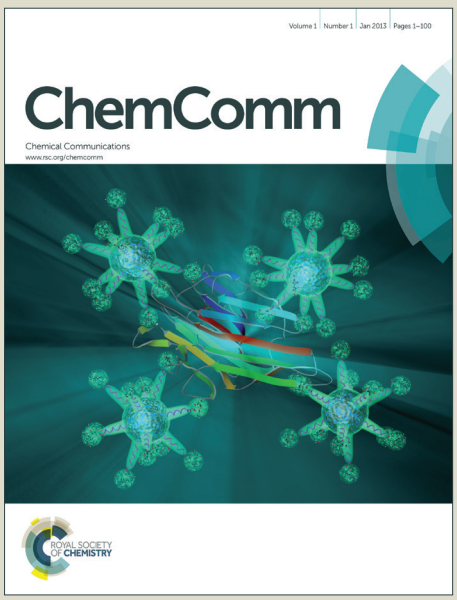

ROYAL SOCIETY OF CHEMISTRY

www.rsc.org/chemcomm

Journal Name

RSCPublishing

COMMUNICATION

One pot multicomponent synthesis of tetrahydropyridines promoted by the aggregates of 6, 6-dicyanopentafulvene supported luminescent ZnO nanoparticles

Cite this: DOI: 10.1039/xoxxoooooox

Received ooth January 2012,
Accepted ooth January 2012

DOI: 10.1039/xoxxoooooox

www.rsc.org/

Meenal Kataria, Subhamay Pramanik, Manoj Kumar and Vandana Bhalla*

Pot shaped fluorescent aggregates of 6, 6-dicyanopentafulvene derivative 4 serve as reactors and stabilizer for the preparation of luminescent ZnO nanoparticles which exhibit high catalytic efficiency in one pot multicomponent synthesis of tetrahydropyridines.

The tetrahydropyridines are important due to their pharmacological and biological activities such as antiviral, antidepressant and antimalarial activities.[1] Therefore, the development of general methods for the easy synthesis of structurally diverse tetrahydropyridine derivatives which are useful for drug discovery process need more attention. Among various methods reported for the synthesis of tetrahydropyridine derivatives *viz* proline mediated cascade Mannich type intramolecular cyclization,[2] palladium catalysed cyclizations,[3] [3+3] annulations of aziridines and allenoates and cyclization of N-allylamino-substituted Baylis-Hillman adducts,[4] one pot multicomponent reactions (MCR)[5] are advantageous due to their atom and synthetic step economy. However, most of the reported one pot multicomponent reactions for the synthesis of tetrahydropyridines require longer reaction time and higher loadings of expensive catalysts. To overcome these drawbacks of multicomponent coupling reactions, it is important to develop an efficient and economical catalytic system which could lead to the formation of tetrahydropyridine derivatives in shorter reaction time. Recently, various types of metal nanoparticles have been utilized as multipurpose promoters for a wide range of synthetically useful reactions.[6] From our laboratory, we also reported the preparation of inexpensive iron oxide nanoparticles from the aggregates of hexaphenylbenzene derivative and their utilization in Sonogashira coupling reactions.[6b] Having done this, we were then interested in the development of an effective and economical catalytic system which could be utilized in one pot three step multicomponent reactions for the synthesis of tetrahydropyridines. For this purpose, non-planar push-pull dicyanopentafulvene is scaffold of our choice as its aggregation properties are still unexplored.[7] Thus, making use of this scaffold, we designed and synthesized β-naphthol appended dicyanopentafulvene (DCF)[8] derivative **4**. We envisaged that DCF derivative **4** having aromatic groups with rotatable C-C and C-N single bonds could exhibit the aggregation induced emission enhancement (AIEE) characteristics.[9] Further, we expected that the presence of soft imine linkages will enhance the affinity of the molecule toward soft metal ions.[10] Interestingly, derivative **4** showed AIEE characteristics and formed pot like fluorescent aggregates in aqueous media and these aggregates exhibited further enhancement of emission intensity in presence of zinc ions. Additionally, these aggregates served as reactors as well as stabilizer for the preparation of luminescent zinc oxide nanoparticles (ZnO NPs) in mixed aqueous media. Though various methods have been reported in the literature for the preparation of ZnO nanostructures but most of these methods suffer from the limitations of multi steps, longer reaction time and use of drastic conditions.[11] Above all, ZnO nanoparticles generated by using these methods are not stable in aqueous media as luminescence of nanoparticles is lost whereas for biological applications, stability in aqueous media is a prerequisite. Thus, the method being reported in the present manuscript for preparation of luminescent ZnO NPs in aqueous media is advantageous over other reported methods in literature (Table S1, ESI†). Further, to our pleasure, small loading (0.5 mol%) of *in situ* generated ZnO NPs exhibited excellent catalytic efficiency in one pot three (*in situ* five) component reactions for the preparation of tetrahydropyridines.[12] To the best of our knowledge this is the first report where the weakly fluorescent aggregates of DCF derivative exhibit ZnO nanoparticle induced AIEE phenomenon and further these *in situ* generated ZnO nanoparticles serve as efficient catalytic system in multi component reactions for the preparation of tetrahydropyridines.

Knoeovenegal condensation between derivative **1** and malononitrile resulted in the formation of 6, 6-dicyanopentafulvene derivative **2a** in 52% yield. Subsequently Suzuki-Miyaura cross coupling between **2a** and **3a** furnished the derivative **2b** in 56% yield which on condensation with β-hydroxynaphthaldehyde **3b** afforded desired product **4** in 85% yield (Scheme 1). The structure of compound **4** was confirmed from its spectroscopic and analytical data (Fig. S32-37, ESI†).

The UV-vis spectrum of derivative **4** in THF exhibits three absorption bands at 320, 390 nm and 450 nm due to π-π* and n-π* transitions. Upon addition of water fraction up to 80% to the THF solution of derivative **4** the intensity of all the absorption bands increased gradually with the appearance of *level off* tail in the visible region (Fig. S1A, ESI†) which suggests the formation of aggregates in aqueous media.

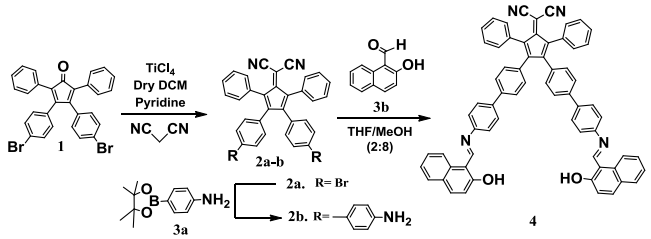

Scheme 1: Synthesis of 6, 6- dicyanopentafulvene derivative **4.**

Further, scanning electron microscopic (SEM) images of derivative **4** in H_2O-THF (8:2, v/v) mixture showed the presence of pot shaped aggregates and the dynamic light scattering (DLS) studies indicate the formation of aggregates having average diameter in the range of 550 nm (Fig. S2, ESI†). The fluorescence spectrum of derivative **4** in pure THF exhibits a weak emissive band at 510 nm (Φ = 0.009) with a small peak at 447 nm when excited at 390 nm. On addition of 80% water fraction, nine and four folds emission enhancement at 510 nm and 447 nm is observed respectively (Fig. S1B, ESI†). The quantum yield (Φ) of emission band at 510 nm gradually increases from 0.009 to 0.09 with increase in the water fraction in the THF solution of **4** (Fig. S3A, ESI†). We believe that the band at longer wavelength corresponds to emission of derivative **4** in the aggregated state (Fig. 1A).[13] Furthermore, an increase in the fluorescence intensity at 510 nm was observed with increasing fraction of triethyleneglycol (TEG) (Fig. S3B(a), ESI†) and also with increasing concentration of compound **4** in THF (Fig. S3B(b), ESI†).

We also carried out the time-resolved fluorescence studies of derivative **4** in pure THF and H_2O-THF (8:2, v/v) mixture and it was found that the average life time (τ_{avg}) increases from 0.78 ns to 2.5 ns on moving from pure THF to H_2O-THF (8:2, v/v) mixture (Fig. S4, ESI†). This result suggests that the decay time of derivative **4** in 80% water fractions is longer than that of **4** in pure THF which implies the formation of ordered aggregates.[14] The time-resolved fluorescence studies monitored at the wavelength 510 nm showed that there is very small difference between fluorescence radiative rate constants[15] (k_f) of derivative **4** in THF (1.15×10^7 s^{-1}) and in H_2O-THF (8:2, v/v) mixture (3.2×10^7 s^{-1}); however, large decrease in case of non-radiative decay constant (k_{nr}) was observed from 1.27×10^9 s^{-1} in the molecular state to 0.36×10^9 s^{-1} in the aggregated state (Table S3, ESI†). These results suggest that the deactivation of nonradiative decay due to restriction in the intramolecular rotational relaxation of the rotors linked to the DCF core in case of derivative **4** is the main reason of the observed emission enhancement in the fluorescence spectrum. The polarized optical microscopic (POM) image of derivative **4** showed birefringence at room temperature, thus, indicating an ordered morphology (Fig.S5A(a), ESI†).

The presence of hydroxyl and imino groups in derivative **4** prompted us to evaluate the binding behaviour of aggregates of derivative **4** toward different metal ions such as Cd^{2+}, Ba^{2+}, Hg^{2+}, Fe^{3}+, Ni^{2+}, Zn^{2+}, Cu^{2+}, Pb^{2+}, Ca^{2+}, Co^{2+}, Ag^{+}, Au^{3+}, $Na^{+,}$ K^{+}, Li^{+}, Pd^{2+}, Cr^{3+}, and Al^{3+} ions as their perchlorate/chloride/or both perchlorate and chloride salts by UV-vis and fluorescence spectroscopy in H_2O-THF (8:2, v/v) mixture. Among the various metal ions tested, the aggregates of derivative **4** showed selective response towards Zn^{2+} ions. The UV-vis absorption studies show the appearance of a new absorption band at 370 nm on addition of Zn^{2+} ions (350 equiv.) to the solution of derivative **4** in mixed aqueous media (H_2O-THF, 8:2, v/v) with an increase in the intensity of *level-off* tail in the visible region (Fig. S5B, ESI†). The band at 370 nm suggests the formation of ZnO NPs.[16] The intensity of absorption band at 370 nm gradually increased with time (180 min). The rate constant for the formation of ZnO NPs was found to be 5.9×10^{-5} s^{-1} (Fig. S6, ESI†). However, no significant change in the absorption behaviour of aggregates of derivative **4** was observed in the presence of other metal ions such as Cd^{2+}, Ba^{2+}, Hg^{2+}, Fe^{3+}, Ni^{2+}, Cu^{2+}, Pb^{2+}, Ca^{2+}, Co^{2+}, Ag^{+}, Au^{3+}, Na^{+}, K^{+}, Li^{+}, Pd^{2+}, Cr^{3+}, and Al^{3+} ions (Fig. S7, ESI†).

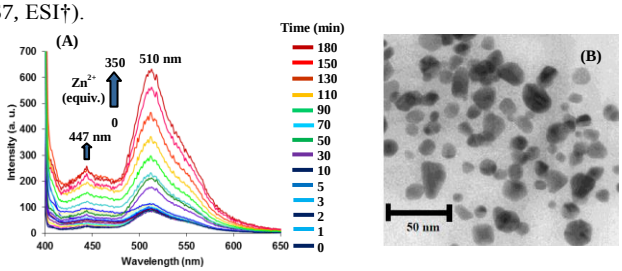

Fig. 1: (A) Time dependent fluorescence spectra of compound **4** (5 μM) showing the response to the Zn^{2+} ions (0-350 equiv.) in H_2O-THF (8:2, v/v) mixture buffered with HEPES; pH = 7.05; λ_{ex}= 390 nm; (B) TEM image of ZnO nanoparticles.

The time dependent fluorescence studies of derivative **4** in the presence of zinc ions (0-350 equiv.) show 6.4 folds enhancement in the emission band at 510 nm (Φ = 0.36) within 180 min with a slight increase in intensity of the emission band at 447 nm (Fig. 1A). The emission enhancement depends on the amount of Zn^{2+} ions added and time interval. Further, on the addition of Zn^{2+} ions into the solution of derivative **4**, the emission spectra showed three emission bands at 457, 480 and 510 nm on excitation at different wavelengths (between 300-345 nm) (Fig. S8A, ESI†).[17] These emission bands overlap with each other and also with the emission band at 510 nm of aggregate **4** in presence of Zn^{2+} ions. The excitation spectra of derivative **4** in the presence of Zn^{2+} ions for the emission at 510 nm showed two peaks at 300 and 378 nm (Fig. S8B, ESI†). These results suggest that localized surface plasmon state of zinc oxide nanoparticles (ZnO NPs) is likely to be the one of the origins of emission band at 510 nm. The detection limit of aggregates of derivative **4** for Zn^{2+} was found to be 95×10^{-8}M (Fig. S9, ESI†). Under the same conditions as used for Zn^{2+} ions, we tested the fluorescence behaviour of aggregates of derivative **4** toward other metal ions such as Fe^{2+}, Cd^{2+}, Hg^{2+}, Pd^{2+}, Fe^{3+}, Cu^{2+}, Co^{2+}, Ca^{2+}, Ba^{2+}, Ag^{+}, Mg^{2+}, Al^{3+}, Li^{+} Na^{+} and K^{+} ions as their chloride and perchlorate salts, but no significant change in fluorescence intensity was observed (Fig. S10, ESI†). Thus, the aggregates of derivative **4** show selective response towards Zn^{2+} ions.

We also carried out the time resolved fluorescence studies of derivative **4** in the presence zinc ions. The fluorescence life time data for derivative **4** in H_2O-THF (8:2, v/v) was obtained by fitting the time resolved curves based on bi-exponential function at 510 nm (Fig. S11, ESI†). In the absence of zinc ions, major fractions of molecules (56%) undergo radiative decay through the fast pathway (τ_1 = 0.74 ns). On the

other hand, in the presence of zinc ions, the major fraction (95%) of the molecules decay through the slower pathway (τ_2 = 9.6 ns). Further, a small increase in radiative rate constant, but a large decrease in non radiative rate constant (from 3.6×10^8 to 0.9×10^8 s^{-1}) was observed in the presence of zinc ions (Table S4, ESI†). These results suggest that the presence of zinc ions further restrict the intramolecular rotation of the rotors which is responsible for the deactivation of nonradiative decay and hence enhancement in emission intensity is observed.[18] All the above results suggest the existence of ZnO NPs induced AIEE phenomenon within the aggregates of derivative **4**. The TEM images (Fig. 1B) of the solution of derivative **4** in the presence of zinc ions showed the presence of spherical ZnO nanoparticles (Fig. S12A, ESI†). The POM image of sample **4** containing ZnO NPs showed birefringence (Fig. S5A(b), ESI†). Further, the confocal microscopy image of compound **4** in the H_2O-THF (8:2, v/v) solvent mixture in presence of zinc ions clearly indicates the presence of luminescent particles (Fig. S12B, ESI†). We also observed that, these *in situ* generated ZnO NPs are visibly stable at room temperature for several months.

To get further insight into the mechanism of formation of zinc oxide nanoparticles, we slowly evaporated the solution of derivative **4** containing ZnO NPs. After 3 days, precipitates were obtained which were filtered and washed with THF to remove organic part. The ^{1}H NMR spectrum of the organic part (Fig. S13, ESI†) obtained after evaporation of THF solution showed the upfield shift of 0.78, 0.31 and 0.27 ppm for hydroxyl, imino and aromatic protons, respectively (Table S5, ESI†). On the basis of above results, we propose that upon addition of Zn^{2+} ions to the solution of aggregates of **4**, Zn^{2+} ions interact with nitrogen atoms of imino groups of derivative **4** and enter into the network of interconnected channels and get reduced to Zn(0) which is further oxidised to stable ZnO by up taking oxygen from water. Further, the SEM image of derivative **4** in the presence of Zn^{2+} ions in H_2O-THF (8:2, v/v) solution showed change in morphology of aggregates of derivative **4** (Fig. S14A, ESI†). Thus, aggregates of derivative **4** functioned as reactors and stabilizing agent for the preparation of stable nanoparticles at room temperature. The effect of pH on the formation of ZnO NPs was studied by zeta potential studies.[19] The zeta potential of ZnO NPs was measured at different pH values after the addition of Zn^{2+} ion to the solution of derivative **4** in H_2O-THF (8:2, v/v). The zero point charge for ZnO nanoparticles was observed at pH 7 and 10.5. ZnO nanoparticles are positively charged between pH 7 to 10.5 and negatively charged between pH 10.5 to 11.5 (Fig. S14B, ESI†). At acidic pH, zeta potential was negative which suggests the partial dissolution of ZnO NPs. These studies suggest that the formation of zinc oxide nanoparticles is more favourable in basic medium.

The powder X-ray diffraction (XRD) studies (Fig. S15, ESI†) of the crystalline residue showed the presence of diffraction peaks located at 2θ values of 31.73, 34.38, 36.22, 47.49, 56.53, 62.79, 66.29, 67.83, 68.98, 72.49, 76.86 which suggests the formation of ZnO nanoparticles.[20] Dynamic light scattering (DLS) data showed the formation of nanoparticles with average diameter in the range of 10-26 nm (Fig. S16A, ESI†). The Raman-scattering spectrum of ZnO nanoparticles showed a peak at 437 cm^{-1} which suggests the formation of spherical ZnO nanoparticles (Fig. S16B, ESI†).[21]

Having done all this, we then planned to examine the catalytic efficiency of the *in situ* generated ZnO NPs in the one pot, three step multicomponent reactions for the synthesis of tetrahydropyridine derivatives. For this purpose we performed one pot reaction of methyl-acetoacetate **6a** (1 mmol), aniline **7a** (2 mmol) and *p*-methoxy benzaldehyde **8a** (2 mmol) in the presence of 0.5 mol % ZnO NPs (100 µl, H_2O-THF, 8:2, v/v) to furnish the target compound **12a** in 91% yield in nearly solvent free conditions (Scheme 2).[22] Additionally, it was found that the ZnO NPs could be reused up to five times without significant loss of their catalytic activity. The scope of this reaction was further explored by using different aldehydes, β-ketoesters and amines (Scheme 2). The results of these reactions summarized in Table 1 suggest that in the presence of only 0.5 mol % of ZnO NPs, the reactions between methyl/ethyl acetoacetate **6a-b**, aniline **7a** and aromatic aldehydes **8a-d** having electron withdrawing or electron donating groups proceed smoothly to furnish the desired products **12a-e** in excellent yields (Table S6, ESI†). Further, the reaction of *n*-butylamine **7b** with methyl acetoacetate **6a** and aldehyde **8a** also went smoothly but moderate yield of **12f** was obtained. Thus, the catalytic efficiency of *in situ* generated ZnO NPs for the synthesis of tetrahydropyridine derivatives is better than other catalytic systems reported in the literature (Table S2, ESI†).[23] All the products were isolated and characterized by ^{1}H NMR, ^{13}C NMR and ESI-MS spectra (Fig. S17-S28, ESI†).

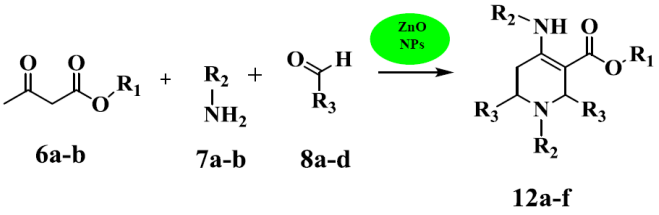

Scheme 2: One pot multicomponent synthesis of tetrahydropyridine derivatives **12a-f** catalysed by ZnO nanoparticles

Table 1: One pot multicomponent reactions of aromatic/aliphatic amines, aromatic aldehydes and β-ketoesters catalysed by ZnO nanoparticles.

Sr. No.	R_1 (6a-b)	R_2 (7a-b)	R_3 (8a-d)	Product 12a-f	Temp.	Time	Yield	Melting point
1.	—CH_3 6a	7a	—OCH_3 8a	12a	RT	2.5 h	91%	189-190°C
2.	—C_2H_5 6b	7a	—CH_3 8b	12b	RT	3h	89%	229-230°C
3.	—CH_3 6a	7a	—CH_3 8b	12c	RT	3h	89%	212-213°C
4.	—CH_3 6a	7a	—H 8c	12d	RT	5h	85%	200-202°C
5.	—CH_3 6a	7a	—NO_2 8d	12e	50°C	9h	80%	255-256°C
6.	—CH_3 6a	nBu— 7b	—OCH_3 8a	12f	50°C	12h	63%	150-151°C

The proposed mechanism for the multicomponent reaction proceeds in four consecutive steps (Scheme 3, ESI†). The reaction steps probably involve the formation of intermediates **9**, **10** and **11** whose structures

were confirmed by ^{1}H NMR (Fig. S29-S30, ESI†). In step-I, nucleophillic addition of amine to β-ketoester furnished the intermediate enamine **9** which reacts with aromatic aldehyde to afford the intermediate **10**. In step-II, the reaction between amine and aromatic aldehyde furnished the intermediate Schiff base **11**. In the final step, intermediate **10** tautomerizes and undergoes intermolecular cyclization with **11** to yield the corresponding tetrahydropyridine derivatives **12a-f**. We have separately synthesized these three derivatives **9**, **10** and **11** which were confirmed by ^{1}H NMR and consequently mixed them to get the tetrahydropyridine derivative **12a**. This proved that the reaction may take place through these three steps with the formation of intermediates **9-11**. We also carried out one pot Mannich reaction of 4-chlorobenzaldehyde, aniline and cyclohexanone (1:1:1) by using the ZnO nanoparticles and product **13** was obtained in 96% yield at room temperature (Fig. S31, ESI†). Therefore, this new catalytic system probably works well for the multicomponent as well as three component reactions.

In conclusion, we designed and synthesized 6, 6- dicyanopentafulvene derivative **4** having β-naphthol groups which formed fluorescent aggregates in aqueous media due to its AIEE characteristics. These aggregates showed high affinity towards Zn^{2+} ions and served as reactors and stabilizer for the preparation of ZnO nanoparticles at room temperature and exhibited ZnO NPs induced emission enhancement. Further, *in situ* generated ZnO NPs showed excellent catalytic activity in one pot, multicomponent reactions for preparation of tetrahydropyridine derivatives, **12a-f**.

M.K. and V.B. are thankful to UGC [ref. no. 42-282/2013(SR)] and CSIR (ref. no. 02(0083)/12/EMR-II) for financial support respectively. We are also thankful to UGC for UPE project. Meenal Kataria is thankful to DST for INSPIRE fellowship.

Notes and references

Department of Chemistry, UGC Sponsored Centre for Advanced Studies-1, Guru Nanak Dev University, Amritsar-143005, Punjab, India.
E-mail: vanmanan@yahoo.co.in

† Electronic Supplementary Information (ESI) available: General data, characterization data, UV-vis and fluorescence studies of derivatives **2a-b**, **4** and tetrahydropyridine derivatives **12a-f**. See DOI: 10.1039/c000000x/

1 Z. Xu, D Cawthon, K. A. McCastlain, H. M. Duhart, G. D. Newport, G. D. H. Fang, T. A. Patterson, W. Slikker, S. F. Ali, *Neurotoxicology*, 2005, **26**, 729.

2 M. Misra, S. K. Pandey, V. P. Pandey, V. Pandey, R. P. Tripathi, *Bioorg. Med. Chem*., 2008, **11**, 62.

3 (a) M. Yoshida, K. Kinoshita and K. Namba, *Org. Biomol. Chem*., 2014, **12**, 2394; (b) H. Tsukamoto and Y. Kondo, *Angew. Chem. Int. Ed*., 2008, **47**, 4851

4 R. Chen, S. Xu, L.Wang, Y. Tang and Z. He, *Chem. Commun.*, 2013, **49**, 3543.

5 X. Li, Y. Zhao, H. Qu, Z. Mao and X. Lin, *Chem. Commun.*, 2013, **49**, 1401.

6 (a) Y. Li, X. M. Hong, D. M. Collard, and M. A. E. Sayed, *Org. Lett.*, 2000, **15**, 2385; (b) S. Pramanik, V. Bhalla and M. Kumar, *Chem. Commun*., 2014, **50**, 13533.

7 (a) A. D. Finke and F. Diederich, *Chem. Rec*., 2014, DOI: 10.1002/tcr.201402060; (b) G. Jayamurugan, J. -P. Gisselbrecht, C. Boudon, F. Schoenebeck, W. B. Schweizer, B. Berneta and F. Diederich, *Chem. Commun*., 2011, **47**, 4520.

8 (a) A. D. Finke, O. Dumele, M. Zalibera, D. Confortin, P. Cias, G. Jayamurugan, J. P. Gisselbrecht, C. Boudon, W. B. Schweizer, G. Gescheidt and F. Diederich, *J. Am. Chem. Soc*., 2012, **134**, 18139; (b) T. L. Andrew, J. R. Cox and T. M. Swager, *Org. Lett.*, 2010, **12**, 5302; (c) G. Jayamurugan, J. -P. Gisselbrecht, C. Boudon, F. Schoenebeck, W. B. Schweizer, B. Berneta and F. Diederich, *Chem. Commun*., 2011, **47**, 4520.

9 H. Tong, M. HäuBler, Y. Q. Dong, Z. Li, B. X. Mi, H. S. Kwok and B. Z. Tang, *J. Chin. Chem. Soc.*, 2006, **53**, 243.

10 (a) A. Ojida, M. Inoue, Y. Mitooka, H. Tsutsumi, K. Sada, and I. Hamachi, *J. Am. Chem. Soc*., 2006, **128**, 2052; (b) V. Bhalla, Roopa, and M. Kumar, *Org. Lett.*, 2012, **14**, 2802.

11 S. K. Park, J. H. Park, K. Y. Ko, S. Yoon, K. S. Chu, W. Kim, and Y. R. Do, *Cryst. Growth Des.*, 2009, **9,** 3615.

12 D. Z. Xu, Y. Liu, S. Shi and Y. Wang, *Green Chem.*, 2010, **12**, 514.

13 X. -H. Jin, C. Chen, C. -X. Ren, Li. -X. Cai and J. Zhang, *Chem. Commun.*, 2014, DOI: 10.1039/c4cc07063a.

14 H. Tong, Y. Hong, Y. Dong, Y. Ren, M. Haussler, J. W. Y. Lam, K. S. Wong and B. Z. Tang, *J. Phys. Chem. B*, 2007, **111**, 2000.

15 (a) Y. Kubota, S. Tanaka, K. Funabiki and M. Matsui, *Org. Lett.*, 2012, **14**, 4682; (b) Y. Ren, J. W. Y. Lam, Y. Dong, B. Z. Tang and K. S. Wong, *J. Phys. Chem. B*, 2005, **109**, 1135.

16 (a) M. S. Hamdy, R. Amrollahi, I. Sinev, B. Mei, and G. Mul, *J. Am. Chem. Soc*., 2014, **136**, 594;.

17 H. -M Xiong, *J. Mater. Chem*., 2010, **20**, 4251.

18 A. Layek, B. Manna and A. Chowdhury, *Chem. Phys. Lett*., 2012, **539,** 133.

19 R. Brayner, S. A. Dahoumane, C. Y.epremian, C. Djediat, M. Meyer, A. Coute, and F. F. Evet, *Langmuir*, 2010, **26,** 6522.

20 A. Mclaren, T. V. Solis, G. Li, and S. C. Tsang, *J. Am. Chem. Soc*., 2009, **131**, 12540.

21 (a) A. Irzh, I. Genish, L. Chen, Y. C. Ling, L. Klein and A. Gedanken, *J. Phys. Chem. C*, 2009, **113,** 32**;** (b) A. Khan, *J Pak Mater Soc.*, 2010, **4**, 31.

22 S. Pal, L. H. Choudhury, T. Parvin, *Mol. Diversity*, 2012, **16**, 129.

23 (a) X. Li, Y. Zhao, H. Qu, Z. Mao and X. Lin, *Chem. Commun.*, 2013, **49**, 1401; (b) H. Tsukamoto and Y. Kondo, *Angew. Chem. Int. Ed*., 2008, **47**, 4851.

